

Appendix to Accompany Snider et al.

Systematic error in velocity:

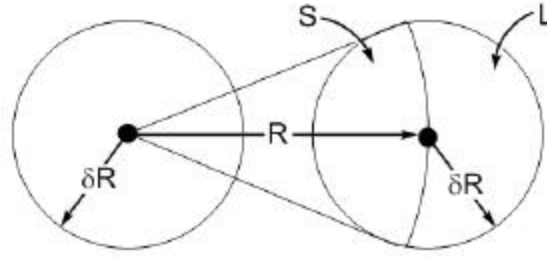


Figure 1: Cartoon of single particle tracking. The centers of the circles represent true particle positions, and the circles represent the error in the location. Fixing the left hand point to be the center, all points in the region labeled S will have apparent distances less than the true distance while all points in L have larger apparent distance. Since L is larger than S by area, the average apparent distance will be systematically too large.

Single particle tracking measurements have a systematic error which causes the average apparent distance that a particle has moved to be larger than the actual distance. This effect becomes more pronounced as the displacement decreases between successive positions. Here we will derive the expression for the systematic error in the measurement of displacement in single particle tracking. As far as we know this phenomena is not discussed, but it may have some consequences for high accuracy tracking experiments. With reference to Figure 1 and choosing a coordinate system centered at the left circle, all points contained by the two circles are given by

$$\vec{p}_1 = (r_1 \sin \mathbf{q}_1, r_1 \cos \mathbf{q}_1) \quad (1.1)$$

$$\vec{p}_2 = (R + r_2 \sin \mathbf{q}_2, r_2 \cos \mathbf{q}_2) \quad (1.2)$$

where 1 refers to the left circle and 2 the right, $r_{1,2} \in [0, dR]$ and $\mathbf{q}_{1,2} \in [0, 2\mathbf{p}]$. Then, the average distance between two randomly selected points is given by integrals over all possible left and right ends. Defining \bar{D} to be the average distance, the integral is

$$\bar{D} = \frac{1}{(2\mathbf{p}dR^2)} \int_0^{2\mathbf{p}} d\mathbf{q}_1 \int_0^{\mathbf{p}} d\mathbf{q}_2 \int_0^{dR} dr_1 \int_0^{dR} dr_2 r_1 r_2 |\vec{p}_1 - \vec{p}_2|. \quad (1.3)$$

This integral is not solvable in closed form; however, we can pull the R out of the

$$\underline{dR}$$

integrand and Taylor expand in terms of $\frac{dR}{R}$, which is hopefully not too large or else other problems will be dominant. When expanding, all terms which contain odd powers of sine or cosine can be ignored because the integral over a full period will be zero. To second order, the contributing terms are

$$\bar{D} = \frac{R}{(2\mathbf{p}dR^2)} \int_0^{2\mathbf{p}} d\mathbf{q}_1 \int_0^{\mathbf{p}} d\mathbf{q}_2 \int_0^{dR} dr_1 \int_0^{dR} dr_2 r_1 r_2 \left[1 + \frac{1}{2} \left(\frac{r_1}{R} \right)^2 \cos^2 \mathbf{q}_1 + \frac{1}{2} \left(\frac{r_2}{R} \right)^2 \cos^2 \mathbf{q}_2 \right]. \quad (1.4)$$

The remaining integrals are trivial and the result is

$$\bar{D} = R \left[1 + \left(\frac{dR}{2R} \right)^2 \right]. \quad (1.5)$$

To check that this result is not just a problem with the expansion, we have also simulated the situation. These straightforward simulations entail choosing two circles of fixed radii separated by a varying distance R to represent the data points and their error. In all cases we choose the radius $dR = 1$ and vary R such that dR/R goes from zero to one, representative of the relative range. Note that a $dR/R = 1/2$ corresponds to the two circles just touching. Then, the distance between a million randomly selected points in each circle is calculated and averaged. The result shown in Figure 2 shows excellent agreement between the calculation and the simulation, although the calculation produces a noticeable but slight underestimate as dR/R approaches one.

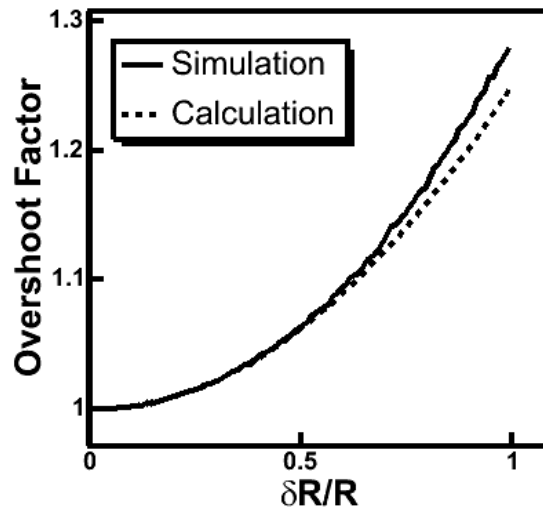


Figure 2: Comparison of simulated and calculated overshoots. The overshoot factor is the ratio of the apparent separation divided by the true separation. A dR/R of one half corresponds to the circles just touching and has an overshoot of 6.25%.

With this systematic error in mind, we calculate the speed of the cargos by plotting the apparent speeds calculated after time spans of 1, 2, ..., 10 frames, where one frame is 7.5s here. Then, we correct the speed using equation (1.5) and vary δR until the corrected speeds do not depend on the time span of the data. With this, the values for the speeds are 70 ± 20 nm/s with $\delta R = 24 \pm 4$ nm for aggregation and 80 ± 30 nm/s with $\delta R = 20 \pm 4$ nm for dispersion. The values of δR are reasonable for these in vivo systems.

Details of the Simulations:

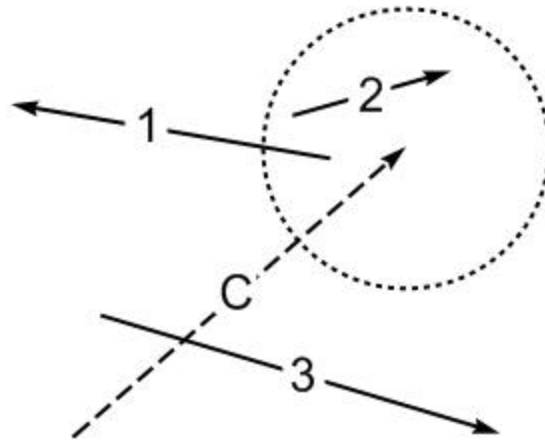


Figure 3: This is a sketch of intersections. The arrows represent actin filaments. The dashed filament, labeled C, has its end radius drawn in and represents the most recently added filament. As defined in the text, C "end intersects" with 1 and 2 but not 3, and C "cross intersects" 3 but neither 1 nor 2.

There are two types of intersections: “cross intersections” where two filaments cross and “end intersections” where a new filament is reachable from the end of the old filament (Figure 3). Using geometry, the computer identifies these intersections as filaments are added during the process of setting up the actin filament network. Call the newly added filament the “current” filament and all others “target” filaments. After each filament addition, the computer examines all target filaments for both cross and end intersections with the current filament and vice versa, and, if necessary, it finds the point on the target filament to which a cargo switching from the current filament will go. Each filament is described by an equation for a line segment. The fact that a filament is a line segment is handled by keeping track of the end points. Determining the existence of a cross intersection is done by solving the equations of the two filaments for their common point and then checking if that common point is on one of the filaments. Note that this also results in the location of the intersection, which is recorded at the same time and used as the transfer point. For end intersections, we consider a circle centered at the filament end point with a radius set to 250 nm to coincide with a cargo. The existence of an intersection is determined by first checking if the endpoints of the target filament are inside or outside of the current filament’s end circle. If exactly one or two endpoints are interior to the circle, then intersection occurs. If both are exterior, then the perpendicular distance to the target filament is found, and if it is less than or equal to the end radius, then an end intersection occurs. If an end intersection is found to occur, then the transfer point is defined as the point on the target filament with the minimum distance to the end of the current filament. Note that it is certainly possible, and fairly common, for a target filament to have both an end and cross intersection. The main simplification made here is that the filament network is fixed. To be applicable to real systems where AFs do move, this fixed approximation means that the time scale on which AFs change is long compared to that on which the cargos move. This is a reasonable approximation since the time scale for AFs change is on the order of several minutes.

Now, we describe the motion of the cargos on the filaments in the simulation. To start, a filament near the center of the simulation cell is chosen at random and a cargo is

placed randomly on it. Then, the cargo takes a step of size 37 nm, corresponding to the size of an MV step¹. First, the computer checks if the cargo has attempted to walk off the end of the filament, and if so it randomly selects an end intersecting filament and switches the cargo onto it. Second, if the cargo remains on the filament, then the code looks for cross intersections on this step. If there are any cross intersections, then the cargo attempts to switch onto each one with success probability p_s , set to 50% for aggregation or 0% for dispersion. Any successful switches immediately move the cargo onto the crossing filament. If no intersection is found or accepted, the original step is accepted, and the process is repeated. Also, while this is going on, the distance between turns is tracked for use in calculating the mean free path, and the position of the cargo is tracked for calculating $\langle r^2(t) \rangle$. Trials are ended after up to 10,000 steps or if the cargo attempts to leave the simulation cell. It is possible, but relatively rare, for a cargo to fall off and be unable to find a new filament on which to travel, and in this case the trial is prematurely ended. Presumably, in the real system, lateral diffusion would eventually allow the cargo to reach a new filament.

Mean Free Path Calculation:

We give the details of our calculation of the mean free path given the distance d_l between filament crossings. Let p_s be the probability to switch filaments at an intersection. Then $q=(1-p_s)$ is the probability to skip switching at an intersection. The probability $P(n)$ to skip $(n-1)$ intersections and then switch at the n th intersection is given by $P(n) = p_s q^{n-1}$. Assuming that the cargo attaches to a filament at an intersection, the distance that it goes along a filament before switching to a new filament at the n th intersection (not counting the intersection where it first got on) is given by nd_l . So the average distance traveled along a filament, i.e., the mean free path (MFP), is given by

$$\begin{aligned}
 \text{MFP} &= \sum_{n=1}^{\infty} n d_l P(n) \\
 &= \sum_{n=0}^{\infty} n d_l p q^{n-1} \\
 &= p d_l \frac{d}{dq} \sum_{n=0}^{\infty} q^n \\
 &= p d_l \frac{d}{dq} \left(\frac{1}{1-q} \right) \\
 &= \frac{p d_l}{(1-q)^2} \\
 &= \frac{d_l}{p}
 \end{aligned}$$

This agrees with the expression given in the text. Here we are assuming that the filament is infinitely long.

Possible optimization between aggregation and dispersion—microtubule searching:

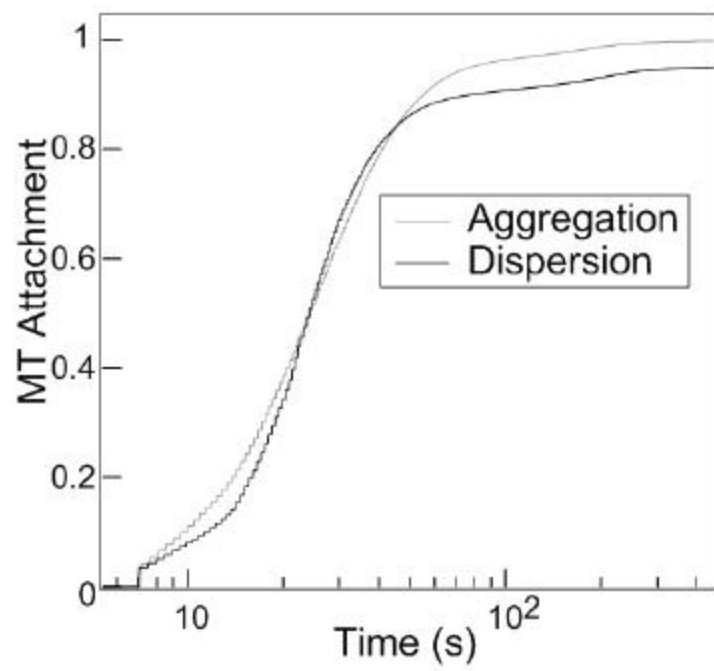


Figure 4: Plot of the fraction of cargoes that have successfully made 15 MT touches versus log time. Errors are smaller than the line width. Aggregation is initially more efficient for times less than 20 s, and then, dispersion is more efficient from about 20-40s. Finally, aggregation is more efficient for times longer than 40s.

For aggregation, the goal is to hop onto a microtubule for subsequent efficient transport to the cell center, so local searching is optimized. Whether this is the case is not directly evident from the current data. To investigate aggregation further, simplified MTs are added to the simulations as parallel lines spaced by 800 nm. A range of distances comparable to the radius (± 125 nm) of a pigment granule is defined around each MT within which a cargo is considered to contact the MT. If only a single cargo-microtubule contact is required, dispersing-type motion is as good or better than aggregation-type motion in finding a microtubule.

However, if multiple cargo-microtubule contacts are required for transfer from the AF to the MT, aggregation-type motion is better. This can be seen by using an arbitrary requirement of 15 contacts. The time required for a cargo to make 15 contacts, or about two passes perpendicularly across a MT, is tracked for 100 realizations with 10,000 cargoes each (Figure 4). In the first 20 s, an aggregating cargo is about 20% more likely than a dispersing cargo to contact any MT 15 times. A dispersing cargo can possibly reach a second set of MTs after 13s, so its rate of contact accelerates, catching up to aggregation after about 20s. Thus, an aggregating cargo contacts the very first MT it reaches 15 times, but a dispersing cargo tends to zip past the first MT and not get 15 contacts until it finds a second MT. Importantly, after a total of about 500s, 5.5% of dispersion cases never contact a MT 15 times but only 0.5% of aggregation cases never do. Thus, fewer aggregating cargoes are 'stranded' on the actin, improving overall transport toward the nucleus. Therefore, aggregation is better than dispersion for allowing multiple contacts between the cargo and the MT and quickly searching locally.

1. **Yildiz, A. et al. Myosin V walks hand-over-hand: single fluorophore imaging with 1.5-nm localization. *Science* 300, 2061-5 (2003).**